Short Communication

Cocoa Pod Husks as Precursors for Biosynthesis of Carbon Dots as Potential Bioimaging Tool

Ashreen Norman[1,2], Ahmad Kamil Mohd Jaaffar[3], Nazzatush Shimar Jamaludin[4], Yuki Shirosaki[5], Norazalina Saad[6] and Che Azurahanim Che Abdullah[1,2,6,*]

[1]Biophysics Laboratory, Department of Physics, Faculty of Science, Universiti Putra Malaysia, 43400 UPM Serdang, Selangor, Malaysia
[2]Nanomaterial Synthesis and Characterization Lab, Institute of Nanoscience and Nanotechnology, Universiti Putra Malaysia, 43400 UPM Serdang, Selangor, Malaysia
[3]Malaysian Cocoa Board, 5 – 7th Floor, Wisma SEDCO, Lorong Plaza Wawasan, Off Coastal Highway, Locked Bag 211, 88999 Kota Kinabalu, Sabah, Malaysia
[4]Department of Chemistry, Universiti of Malaya, 50603 Kuala Lumpur, Malaysia
[5]Department of Materials Science, Faculty of Engineering, Kyushu Institute of Technology, Tobata Campus, 1-1 Sensui-cho, Tobata-ku, Kitakyushu-shi, Fukuoka, 804-8550, Japan
[6]UPM-MAKNA Cancer Research Laboratory, Institute of Bioscience, Universiti Putra Malaysia, Serdang, Selangor, Malaysia

(*) Corresponding author: azurahanim@upm.edu.my

Abstract

Recent zero-dimensional carbon dots (CDs) have dominated the world of nanomaterials due to their ease of synthesis and nature of their precursors. The aim of this study is to synthesize, characterize and evaluate cytotoxicity of CDs from agricultural waste CPH for its potential use in the bioimaging field. The TEM analysis and particle size distribution curve revealed that the particles had a diameter of 10-30 nm, sphere-shaped and exhibited lattice fringes with a d-spacing of 0.196 nm. XRD analysis revealed a broad peak at $2\Theta = 20.71°$, indicating the existence of carbon. FTIR confirmed the presence of multiple functional chemical groups on the surface of the CPH CDs consist of C=O, N–H, C–N, and C–O–C. Due to the electronic transition's characteristic of CDs, the UV-Vis absorption spectrum revealed two distinct peaks at 235 and 293 nm. PL spectra of CPH CDs revealed a red shift in the emission peak from 400 to 410 nm as the excitation wavelength increased from 320 to 380 nm. We used brine shrimp and human colon adenocarcinoma cells (Caco2) in vitro to determine the cytotoxicity of CPH CDs. In terms of brine shrimp assay, we found that 0.001 mg/ml showed lower lethality percentage with 57.93 ± 9.77 %. The cytotoxicity of CPH CDs was assessed in vitro using the MTT assay and Caco2 cell line's viability decreased with increasing concentration (IC50 = 155 ug/ml). Due to their favorable properties and low cytotoxicity, CPH CDs have the potential to be used as bioimaging tools.

Keywords: *Carbon dots, Cocoa pod husks, Brine shrimp assay, Bioimaging, Natural precursors.*

1. INRODUCTION

Carbon dots (CDs) are one of several nanomaterials that have recently captured the attention of researchers. CDs are quasi-spherical and have a diameter of less than 10 nanometers. Additionally, they are referred to as carbon nanodots, graphene quantum dots, or carbon quantum dots [1]. CDs have a wide range of applications in medicine, including in-vitro cell imaging [2], theranostic application [3], vitamin B12 sensing [4], and as antibacterial agents [5]. Additionally, CDs have been used to

detect pesticides in water [6], as well as metal ion sensors [7]. Numerous studies have been conducted on how CDs are manufactured in this technological age by utilizing natural resources. Bhamore and colleagues [8] used the *Manilkara zapota* fruit to create a full spectrum of colourable compact discs. The solution was treated with a variety of acids, including phosphoric and sulphuric acid. When tested on HeLa cells, the product was found to be relatively non-toxic. Ramanarayanan & Swaminathan [9] used the hydrothermal method to create CDs from guava leaves in another experiment. They synthesized CDs had photocatalytic activity for the degradation of methylene blue dye. Additionally, Diao and colleagues [10] demonstrated that the CDs obtained could detect Fe^{3+} and H^+ using the plant *Syringa oblata* Lindl. Another study in 2018 had successfully produced CDs using coffee bean shells where it had displayed its ability in imaging cellular nuclei and tumours in vivo [11]. These experiments demonstrated that CDs with desirable properties can be synthesized from relatively uncomplicated organic starting materials. Additionally, the entire study consists of green synthesized CDs created using simple bottom-up techniques. Malaysia is home to a diverse range of major industries. One of them is agriculture. Our agricultural industry generates a great deal of waste. Biomass is known as renewable energy from plants and animals. In literature, there are many instances where biomass has been employed to develop CDs with various applications, summarized in Table 1. These wastes have the potential to be converted into functional nanomaterials.

The CDs used in this study are made from cocoa pod husks (CPH). It is scientifically referred to as *Theobroma cacao*. It originated in Latin America and has been planted throughout the Americas, Asia, and Africa [17]. Concerns arise because the cocoa industry generates a large amount of waste each year [18].

Table 1. Various biomass from plants and animals as precursors of carbon dots.

Precursors	Method	Application	References
Babassu coconut	Hydrothermal	Sensor for specific ion species	[12]
Soymeal	Microwave and hydrothermal	Printing ink	[13]
Jackfruit and tamarind peel	Hydrothermal	Antitumour	[14]
Black pepper	Solvothermal	Imaging of ascorbic acid	[15]
Coconut water	Hydrothermal	Fluorescence detection of heavy metal ions	[16]

Between 2018 and 2019, the world's cocoa production totaled 4.8 million tons according to the International Cocoa Organization's website. CPH is a significant waste stream in the industry. CPH accounts for 75% of all fruit [19]. Around 923,000 kg CPH are disposed of in Malaysia following the treatment of cocoa beans [20]. CPH is composed of three layers: the epicarp, the mesocarp, and the endocarp [21]. The chemical composition of CPH is shown in Table 2. Typically, CPH is extracted and disposed of as solid waste. Regrettably, CPH has the potential to act as a vector for both human and animal pathogens of *Phytophthora spp* [22, 23]. Additionally, CPH is a source of enzymes such as lipase [24]. Also, phytochemical screening has revealed that the CPH contains polyphenols such as tannins, alkaloids, and saponins. Polyphenols protect against a variety of diseases, including coronary heart disease, cancer, and neurodegenerative disorders. Polyphenols are well-known for their protective properties. Additionally, CPH

Norman, et al.

exhibited antimicrobial activity against *Salmonella choleraesuis* and *Salmonella epidermidis*. The antimicrobial mechanism of action was ascribed to the phenols' ability to penetrate the bacterial cell wall [25]. CPH has an extremely advantageous chemical composition and can be used as a suitable and alternative precursor for CDs. Additionally, the composition of CPH poses no cytotoxicity risk to surrounding cells during bioimaging.

Table 2. Chemical composition of CPH

Chemical composition	Percentage (%)
Ash	9.10
Protein	5.90
Crude Fiber	22.6
NDF	61.0
ADF	50.0
Nitrogen-free	62.2
Crude fat	1.20
Cellulose	35.0
Hemicellulose	11.0
Lignin	14.6
Pectin	6.10
Ca	0.32
K	3.18
P	0.15
Mg	0.22

Adapted from Campos-Vega *et al.,* [21].

CDs outperform quantum dots. The latter has several disadvantages, including time-consuming preparations and a higher toxicity level [6]. Chemical ablation, electrochemical processing, microwave treatment, ultrasonic treatment, pyrolysis, and hydrothermal treatment are all methods for producing these nanoparticles [26]. Each method has its advantages and disadvantages. The bottom-up approaches such as the hydrothermal and microwave methods have their merits. This includes simplified preparation, straightforward control of reaction parameters, economical, and sustainable operations. Acids are sometimes added to the precursors. As a result, functional groups such as hydroxyls, carboxyl, and carbonyls are formed. Hydrolysis and oxidation reactions result in the formation of these functional groups [27]. Bottom-up methods has a high

flexibility in terms of its precursors and synthesis routes instigating many studies on CDs with these methods [28]. On the other hand, top-down methods synthesize carbon materials (graphite, carbon fibers, nanotubes, and fullerenes) in highly acidic environment leading to a more complex and time-consuming production of CDs [29]. Hence, bottom-up methods are usually desirable converts biomass or any organic matter into desired size of CDs [30].

Numerous CDs have been synthesized in recent years. CDs have been proposed for use in biomedicine applications due to their biocompatibility and tunable fluorescence. Numerous studies have been conducted to ascertain its cytotoxicity. The MTT assay was used to determine the adhesion of CDs coated with chitosan and Gum Tragacanth to primary human umbilical vein endothelial cells (HUVEC). The CDs were found to enter cells safely and were stained blue. This demonstrates that CDs were biocompatible and suitable for bioimaging [31]. Additionally, CDs synthesized from baked lamb demonstrated excellent biocompatibility when used with a human liver cancer cell line known as HepG2 cells. CDs were discovered in HepG2 cells and emitted fluorescence in a variety of colors. Additionally, the level of cytotoxicity was low even when the CDs were increased to 2 mg/mL and the cells were incubated for 4 hours [32]. When tested against various cell lines, CDs derived from natural precursors retain their optimal properties. CDs are ideal for bioimaging and cell tracking because they pose no threat to the surrounding cells of a living organism.

Ricardo *et al.* [33] conducted the first comprehensive study of the life cycle assessment (LCA) of CDs. The evaluation compared hydrothermal, and microwave assisted treatment, with the latter proving to be significantly more sustainable. Additionally, the study determined that the primary environmental impact is a result of the type of precursor used. As a result, the

microwave method was chosen for this work and the precursor was CPH, a waste product of the cocoa industry. This method is both effective and economical in terms of avoiding the use of harmful chemicals. Also, this method reduces the production time of CDs [34]. It demonstrates that organic matter of all types can be used to create functional products using simple and low-cost methods that are environmentally friendly. Due to its high concentration of cellulose, hemicellulose, and lignin CPH is a suitable biomass material to be used as a precursor in the making of CDs. In a study by Wu and colleagues [35], it was that high percentile of hemicellulose, cellulose and lignin content was of corn cobs makes it suitable to synthesis CDs. Furthermore, the number of articles published related to cocoa wastes and nanoparticles increased gradually from 2015 to 2020. This is evident from the data provided in Lens.org and is tabulated in Figure 1. Therefore, this study is relevant to the current research that has been carried out in repurposing wastes from the cocoa industry. The structural and optical properties of the CPH CDs were investigated using TEM, XRD, FTIR, UV-Vis, and PL in this study. Additionally, the cytotoxicity of CPH CDs will be determined using an aquatic animal model known as brine shrimps.
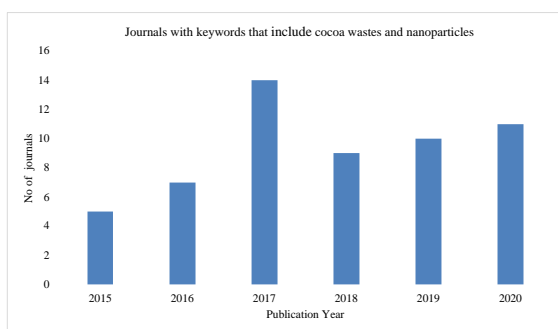

Figure 1. The table shows the number of journals published from the year 2015 till 2020 which included keywords of cocoa wastes and nanoparticles (Source: lens.org).

2. MATERIALS AND METHODS

Cocoa pod husk (CPH) was obtained from Malaysian Cocoa Board, Negeri Sembilan, Malaysia. Throughout the experiment, laboratory distilled water was used. CPH was dried in an oven for approximately 48 hours. The pod was then ground into a fine powder. To begin, approximately 2g of CPH powder was homogeneously mixed in 40 mL of distilled water. Following that, the solution was sonicated for 10 minutes before being microwaved for 3 minutes at 550 watts. After cooling, the crude products were centrifuged at 6000 rpm for 10 minutes and filtered through Whatman filter paper followed by a 0.2 m syringe filter. The procedure is summarized in Figure 2. Until further experimentation, the purified CPH CDs solution was kept at 4°C.

Figure 2. Preparation of CPH CDs by microwave irradiation method.

To study the morphology of CPH CDs, image of these particles was performed with a Transmission Electron Microscopy (JEM-F200 Multi-purpose Electron Microscope, Japan). The structure of CPH CDs was analyzed with X-ray diffraction equipment (Rigaku, Japan). The prepared CPH CDs' FTIR spectra were analyzed using a Fourier transform infrared spectrum (FTIR-spectrum 400, Perkin Elmer, USA) over a spectral range of 1000 to 4000 cm^{-1}. UV-Visible absorption spectrum of CPH CDs were recorded using a quartz cuvette ((Lambda 35 UV/Vis Spectrophotometer, Perkin Elmer, USA). Additionally, the optical properties of CPH CDs were analyzed using photo-luminescence spectroscopy (Tecan Spark, Switzerland) with an excitation wavelength range of 32-380 nm.

The brine shrimp bioassay (hatching and lethality) was performed in the manner described by Naidu *et al.* [36] with minor

modifications to determine the cytotoxicity of synthesized CPH CDs. The model organism was *Artemia nauplii* (brine shrimp eggs). The hatched and umbrella stage brine shrimps were calculated for the hatching assay. Brine shrimps were incubated in solutions containing 0.001 mg/mL, 0.01 mg/mL, 0.1 mg/mL, and 1 mg/mL of CPH CDs. Ten to fifteen brine shrimp cysts were placed in each well of the 96-well plate. Following that, each well was filled with 200 liters of saltwater containing CPH CDs. After 24 hours of exposure to the CPH CDs solution, the hatching percentage was calculated. For the lethality assay, brine shrimp cysts were allowed to hatch for 24 hours before calculating their percentage of lethality. The hatching and lethality rates were calculated as follows:

The hatching percentage (%) is (Equation 1)

$$\frac{No.\ of\ hatched,\ include\ umbrella\ stage}{Decapsulated\ full\ cysts + Hatched}\ x\ 100\%.$$

The lethality percentage (%) is (Equation 2)

$$\frac{No.\ of\ dead\ brine\ shrimp}{Dead + living\ brine\ shrimp}\ x\ 100\%$$

The median lethal concentration or else known as LC_{50} is the result of when half of the brine shrimp population is killed (Hamidi *et al.,* 2014). LC_{50} of the tested synthesized compounds was ascertained from the concentration and linear regression from the graph. The data obtained from the brine shrimp assay were analyzed using Microsoft Excel, Prism 8.0 (Graph pad, USA) and Origin 2021 version 9.8 (Origin Lab, USA).

The cell culture media used were as follows; α Minimum Essential Medium (α-MEM) with L-Gln, without Ribonucleosides and Deoxyribonucleosides were purchased from Nacalai Tesque, Inc whereas Gibco™ Dulbecco's modified Eagle's medium (DMEM) were purchased from Thermo Fisher Scientific (Waltham, MA, USA). MTT (3-[4,5-dimethylthiazol-2-yl]-2,5-diphenyltetrazolium bromide) was purchased from Ekear; Shanghai, China.

Caco2 cells [HTB-37™□] (human colon adenocarcinoma cells) were used in this study. The cells were purchased from the American Type Culture Collection (ATCC; Manassas, VA, USA). Caco2 cells were cultured in DMEM culture media. The culture media were supplemented with 10% (v/v) fetal bovine serum (FBS) and incubated at 37°C in 5% CO2 incubator (Thermo Fisher Scientific, USA). The cells were cultured in T-25 sterile tissue culture-treated flasks (Corning, USA) with initial density of 5×10^5 cells/mL. The cells were passaged every two or three days or when the cells were 80-90% confluent.

Cytotoxicity refers to the ability of chemicals synthesized in the laboratory, naturally occurring toxins, or immune mediator cells to kill. The MTT (3-[4,5-dimethylthiazol-2-yl]-2,5-diphenyltetrazolium bromide) assay is one of the parameters used to determine cytotoxicity. MTT assays were performed using human colon adenocarcinoma cells (Caco2 cells). Caco2 cells were cultured at a concentration of 3×10^3 cells/ml and plated (100µl/well) onto 96-well plates. Each well was then incubated for 72 hours with the diluted ranges of sample extracts; 500, 250, 125, 75, and 25 (µg/ml). MTT solution was added to the cells at the end of the incubation period and incubated for an additional 3 hours in the incubator. After completing the solubilization of the purple formazan crystals with DMSO, the Optical Density (OD) of the plant extract was determined using an ELISA reader set to 570nm. Cytotoxicity was quantified as the drug concentration that inhibited cell growth by 50% (IC_{50} value) using the following formula (Equation 3):

$$Cell\ viability = \frac{Absorbance\ sample\ (mean)}{Absorbance\ control\ (mean)}\ x\ 100$$

After the determination of the percentage of cell viability, graphs were plotted with the percentage of cell viability against their respective concentrations. The data

obtained from MTT assay were analyzed using Microsoft Excel, GraphPad Prism 8.0 (Graph pad, USA) and Origin software 2021 version 9.8 (Origin Lab, USA) and Image J software version 1.8.0

3. RESULTS AND DISCUSSION
3.1. Physicochemical Properties of CPH CDs

The morphology and size distribution of CPH CDs were assessed with TEM. The results are shown in Figure 3. The TEM results showed that the CPH CDs in Figure 3 (a) were clustered together and are shaped spherically. Green synthesis of CDs usually exhibits spherical shape as exhibited when CDs were made from arrowroot powder [37] and fish scales [38]. Further in-depth analysis, at 10 nm, showed crystalline structures of CPH CDs with lattice parameters of 0.196 nm as seen in Figure 3 (b). According to Ganesan *et al.*, [39], such structures resemble the crystal phase of graphene. By arbitrarily choosing the number of particles, it was found that nearly 72% had a diameter of 10 to 30 nm as shown in Figure 3 (c).

The CPH CDs in Figure 4 show the XRD results which displayed a broad peak of $2\theta = 20.71°$. There is no indication of its crystalline nature. The results indicated that the CPH CDs consist of amorphous carbon as supported by previous research [40]. According to Atchudan *et al.,* [41], CDs made from natural resources usually will have an amorphous structure or a crystalline core with an amorphous outer.

CPH CDs contain diversified chemical compounds. It was assumed that as characterized by FTIR spectroscopy, the surface of CPH CDs could have enormous functionalities. In Figure 5, the peak observed around 3200 to 3300 cm^{-1} is indicative of the vibration stretching of the O-H and/or N-H bond. This stipulates CPH CDs are hydrophilic [2]. Besides that, peaks located around 1725 cm^{-1} and 1040 cm^{-1} corresponded to C = O and C – O stretching vibrations respectively [6].
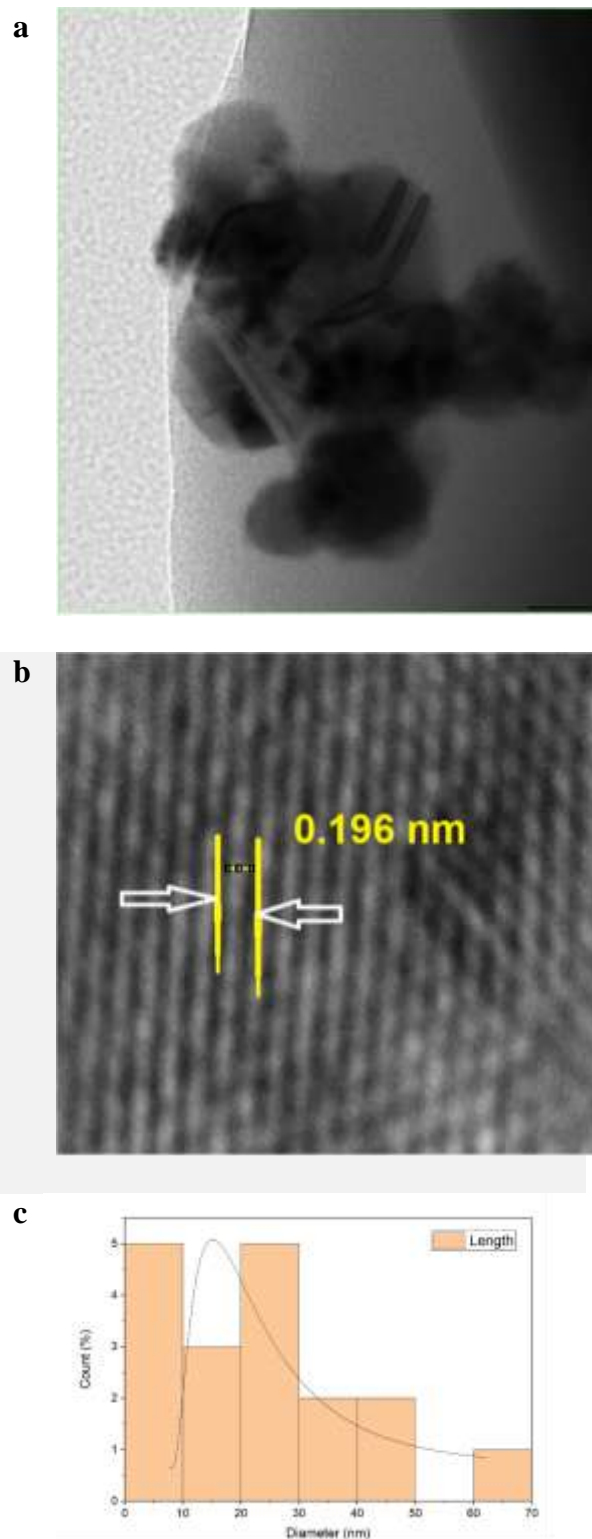
Figure 3. (a) TEM of overlapping spherical shapes of CPH CDs at 50nm (b) Interlayer lattice spacing of CPH CDs at 10 nm (c) Histogram of CPH CDs average diameter
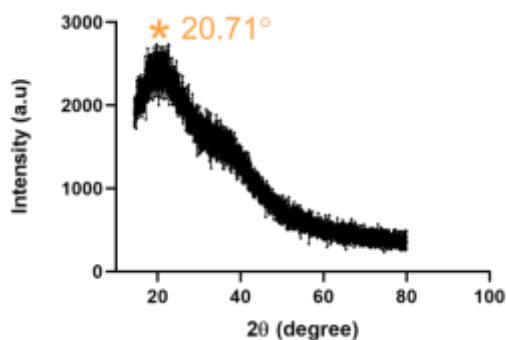
Norman, et al.

Figure 4. *XRD analysis of CPH CDs.*

Also, the functional group C = O shows the stretching vibration of COOH groups around the frequency of 1600 - 1700 cm^{-1}. By referring to the FTIR results, the presence of C = O group and other carboxylate groups increases the presence of oxygen on the surface. The increase in oxygen groups leads to an increase in surface defects. If there are defects, the excitons will be trapped giving a red-shifted emission [42]. The peak found around 2920 cm^{-1} is related to the vibrations of C-H stretching [2,5]. The presence of these functional oxygenated groups gives rise to soluble properties of the CPH CDs [27]. All FTIR features contribute to the outstanding solubility of CPH CDs. The CPH CDs were found to be very soluble at 1mg/mL due to the presence of carboxylate groups. It is suggested that the CPH CDs prepared will be useful for further modifications and biological applications.
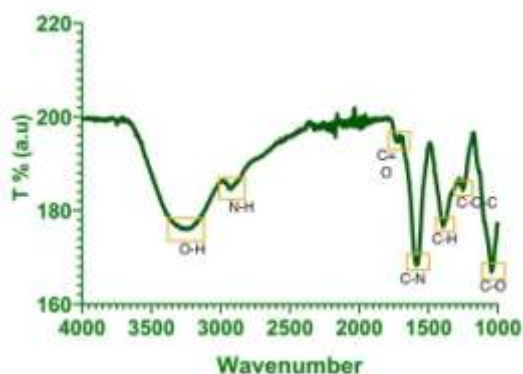
Figure 5 *FTIR spectrum of CPH CDs from 1000 cm^{-1} to 400 cm^{-1}*

3.2. UV-Visible Absorption and Photoluminescence of CPH CDs

The optical properties of the prepared CPH CDs were determined using UV-visible (UV-Vis) absorption and photoluminescent (PL) spectra. These are depicted in Figure 6. Due to the C = O bonds, the optical absorption peak of CPH CDs was observed at 214 nm in the ultraviolet region, as shown in Figure 6. The electronic transitions n - π* also contributed to this peak. A peak was also detected in the range of 281 nm due to the C = C (π-π*) present in CPH CDs [43]. The presence of these electronic transitions indicates that functional groups exist on the surface of CPH CDs. Additionally, the findings indicated that the specific peaks indicated that CPH CDs were successfully formed using a simple microwave method.
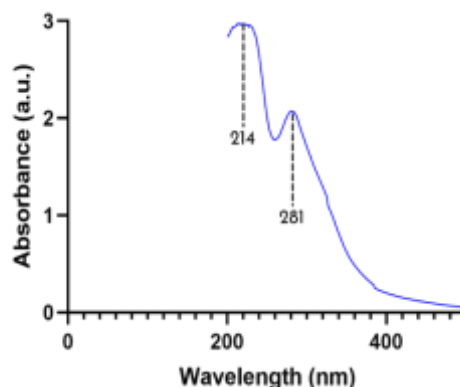

Figure 6. *UV Visible absorption spectrum of CPH CDs*

The band gap of the CPH CDs was calculated from the UV-Vis absorbance spectrum using the Tauc plot. The Tauc plot illustrates the relationship between photon energy and $(ahv)^2$. The energy band gap was calculated using the linear region of the absorbance photon energy (hv) versus ahv^2 plot. As illustrated in Figure 7, the CPH CDs have a band gap of 4.38 eV. Our findings corroborate prior research conducted by Jumardian and colleagues [44]. Their findings indicated that with increased laser ablation time (2, 3 hours), both the direct and indirect optical energy gaps decreased. Sekar and Yadav [45],

reported a bandgap of 3.30 eV for their bare CDs made from gum ghatti powder. Additionally, Yu and colleagues [46], discovered a bandgap of 4.10 eV for CDs with an innate carbon core. According to a study conducted by Sutanto and colleagues [47], the energy bandgaps of compact discs increased as microwave power increased. Additionally, it was stated that electrons need more energy to be liberated from the valence band and into the conduction band at higher energy bandgaps. This study uses 550 Watt to generate the CPH CDs that result in these higher energy bandgap carbon nanomaterials.
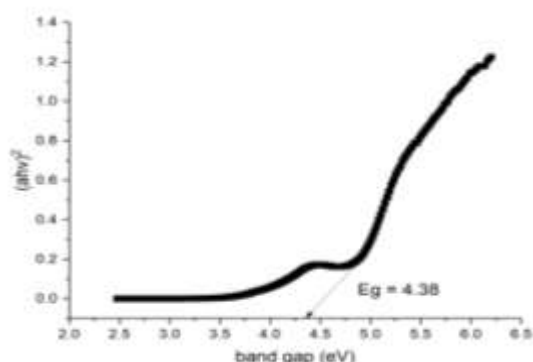
Figure 7. *Tauc plot of CPH CDs*

When exposed to UV light, the aqueous solution of the CPH CDs was fluorescent green. The result indicates that the excitation-dependent PL characteristic of CPH CDs is accompanied by a broad PL peak because of quantum confinement and edge deformities. From our preliminary data, we found that at a higher pH, the emission wavelength is at maximum. Figure 8 showcases the fluorescence spectra of CPH CDs when excited at different wavelengths. CPH CDs display the wavelength-dependent characteristics. The nanomaterials were excited from 320 nm to 380 nm. The maximum emission wavelength of 400 nm was achieved when excited at 320 nm. This discovery demonstrates that CPH CDs have the potential to be used as fluorescent detectors in bioimaging applications. The overall trend indicates that as the excitation wavelength is increased, the peaks redshift

due to photon reabsorption. CPH CDs have an interconnected carbon core structure with functional groups on the surface and on the edge [5]. The PL property is dependent on the particle size distribution of the CPH CDs. The various sizes of the CPH CDs correspond to the amount of energy excited by a particular wavelength [48]. As shown in Figure 8, the presence of $C = O$ and other carboxylate groups increase the amount of oxygen on the surface. An increase in the number of oxygen groups results in an increase in the number of surface defects. As a result of the defects, the excitons are trapped, resulting in a red-shifted emission [42]. This is demonstrated clearly in Figure 8, where the emission peaks turn red after 400 nm. Quantum confinement, emissive traps, and the electronic conjugate structure of nanomaterials all contribute to CPH CDs emission [49].
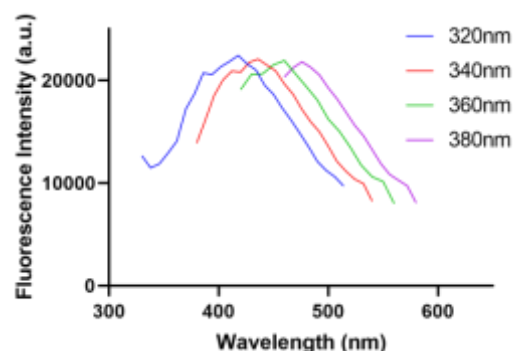

Figure 8. *Photoluminescence result of CPH CDs*

3.3. Brine Shrimp Lethality Assay

CPH CDs are considered an environmentally friendly and non-toxic alternative for a variety of applications due to their non-toxicity. Emphasis is placed on *in-vitro* and *in-vivo* biological systems. A brine shrimp assay was used to determine the nanotoxicity of as-synthesized CPH CDs. The primary objective of the test is to definitively determine whether CPH CDs are well-suited for use as biomedical imaging tools. Additionally, to ensure that no potentially harmful cytotoxic effects are induced. The assay was carried out for the

Norman, et al.

specified time point interval using brine shrimp treated with varying concentrations of CPH CDs. As shown in Figure 8, the lethality percentage increases after 24 hours, cyst survival decreases after that time. At CPH CDs concentrations of 0.001 mg/mL, brine shrimps had a higher survival rate than standard saltwater solution. At 0.001 mg/mL, the lethal concentration is 57.93 ± 9.77 %. By comparison, the lethality of a standard saltwater solution was 61.46 ± 5.59 %. This is a slightly higher value than the value obtained when the concentration was 0.001 mg/mL. As shown in Table 2, the brine shrimps that could hatch were extremely active. Additionally, at concentrations of 0.01 mg/mL and 0.1 mg/mL, *Artemia nauplii* has negligible survival capabilities. At 1 mg/mL, the lethality percentage is 71.18 ± 13.42 %. The majority of those found at this concentration died immediately, even after only 24 hours. In Table 3, the hatching rate is trending downward. Within 24 hours, numerous cysts hatched, and some developed into the umbrella phase. Concentrations of 1 mg/mL resulted in the highest hatching percentage, followed by 0.01 and 0.1 mg/mL.
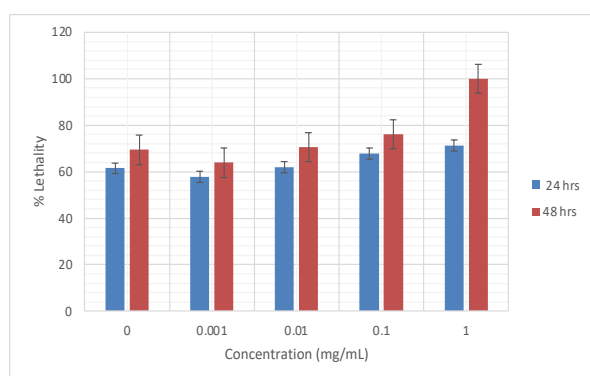

Figure 9. *The bar diagram shows the mortality rate at 24 and 48 hours of brine shrimp cysts treated at various concentrations of CPH CDs.*

After 24 hours, at a concentration of 1 mg/mL, it has the highest hatching percentage of 71.18 13.42 %.

Table 3. *Hatching percentage of brine shrimps' cysts when treated with different concentrations of CPH CDs. Hatching data was obtained after 24 and 48 hours.*

Hatching (%) of test samples		
Concentrations (mg/mL)	24 hours	48 hours
0	61.46 ± 5.59	69.46 ± 8.99
0.001	57.93 ± 9.77	63.89 ± 9.20
0.01	61.89 ± 5.66	70.63 ± 14.56
0.1	67.74 ± 9.71	76.04 ± 7.99
1	71.18 ± 13.42	100 ± 0.00

At this concentration, it was observed that the majority of brine shrimp developed into the umbrella stage. At a concentration of 1 mg/mL, development was halted (Table 3 (g) and (h)). The shrimps disintegrated due to the high concentration of CPH CDs. This can be seen in the images in Table 3 at a concentration of 1 mg/mL. This could be because of the persistence of *Rhizopus sp* fungi isolated from cocoa pods in a previous study (Jimat *et al.*, 2015). Additionally, the brine shrimps hatched at lower concentrations and were extremely agile in the sample. Different CPH CDs concentrations promote the hatching of *Artemia nauplii*, but their survival after 24 hours is dose dependent. CPH CDs containing polyphenols have shown antioxidant properties *in-vitro* [50]. CPH contains nutrients that stimulate the hatching of cysts. However, depending on the dosage of CPH CDs, the brine shrimps either live normally or are suspended in their umbrella phase. The LC_{50} of CPH CDs was determined using the linear regression equation depicted in Figure 4. CPH CDs have an LC_{50} of 1.33 mg/mL. Mayer's toxicity index classifies a sample as toxic if the LC_{50} value is less than 1.0 mg/mL. The LC_{50} value for CPH CDs indicates that they are not toxic in this regard. When CPH CDs are used in living cells, low concentrations such as 0.001 mg/mL, 0.01 mg/mL, and 0.1 mg/mL are non-toxic in comparison to 1 mg/mL. A low dosage is sufficient for biomedical applications. This

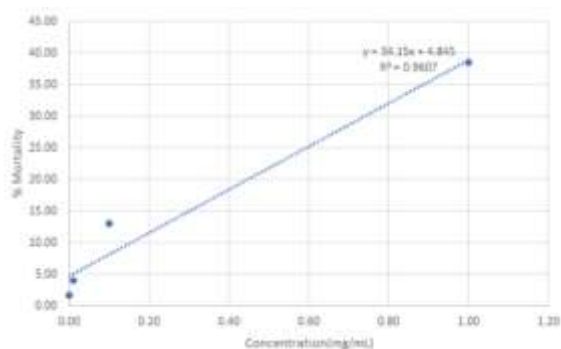will facilitate the body's effective excretion of the nanoparticles as well.

Figure 10. *Mortality percentage and concentration for brine shrimp assay immersed in different concentrations of CPH CDs.*

Concentration	24 hours	48 hours
0.001 mg/ml	a) The cysts above were just hatched from their eggs.	b) Development of the cysts into its mature stage.
0.01 mg/ml	c)The brine shrimp is at its early stage at 24 hours.	d) The brine shrimp is at a mature stage and some of it seemed lifeless due to limited nutrition
0.1 mg/ml	e) Brine shrimp was at its early stage and observed to be very active	f) Cysts have entered a matured stage. In the picture shown, the cysts were observed to be lifeless with limited movements.
1 mg/ml	g) The cysts successfully hatched from its eggs but does not seem to be active. Most of it fell prey to death instantaneously once hatched.	h) Cysts are suspended in the liquid of the sample with no movement. At a high concentration, they are not able to survive.

3.4. MTT Assay

The MTT assay was used to assess CPH CDs' cell viability and potential apoptotic effect on the human colon adenocarcinoma cells (Caco2). Cancerous cells were cultured in CPH CDs at concentrations ranging from 25 to 500 µg/ml for 72 hours, as shown in Figure 11 (a to e), resulting in a significant reduction in cell viability in a dose-dependent manner. The synthesized CPH CDs inhibited Caco2 cells by 50% (IC_{50}) at a concentration of 155 µg/ml, demonstrating the anti-proliferative and apoptotic effect of CPH CDs in human colon adenocarcinoma cells. A similar finding was reported by Basak *et al.* [51], who discovered that Aloe vera whole leaf extract may inhibit the growth of MCF 7 breast cancer cells. Aloe vera contains aloe-emodin, aloin (barbaloin), anthracene, and emodin compounds, as well as phytochemicals such as alkaloids, phenols, and flavonoids, according to the literature [52, 51]. As a result, the cytotoxicity of Aloe vera-derived CDs has been increased. CPH contains phenol and it acts as an antimicrobial compound which has been analysed by Rachmawaty and coworkers [53]. Hence, this property of CPH is suitable to be used as precursor for green synthesis of CDs in the potential treatment of cancer cells and as well as bioimaging. The Caco2 viabilities were 14.61% ± 0.08, 44.84% ± 0.14, 52.16% ± 0.06, 60.82% ± 0.05 and 63.76% ± 0.07 for the CPH CDs concentration of 500 µg/ml, 250 µg/ml, 125 µg/ml, 75 µg/ml, and 25 µg/ml,

Norman, et al.

respectively as indicated by the representative optical images figure 11 (f).
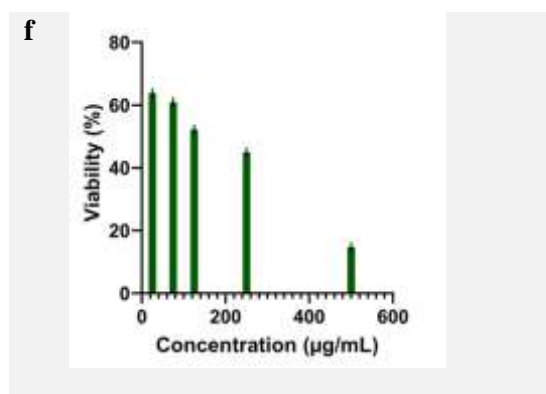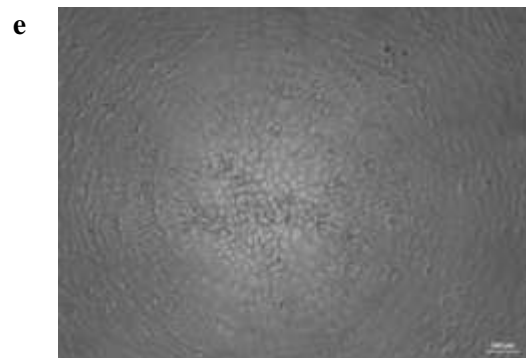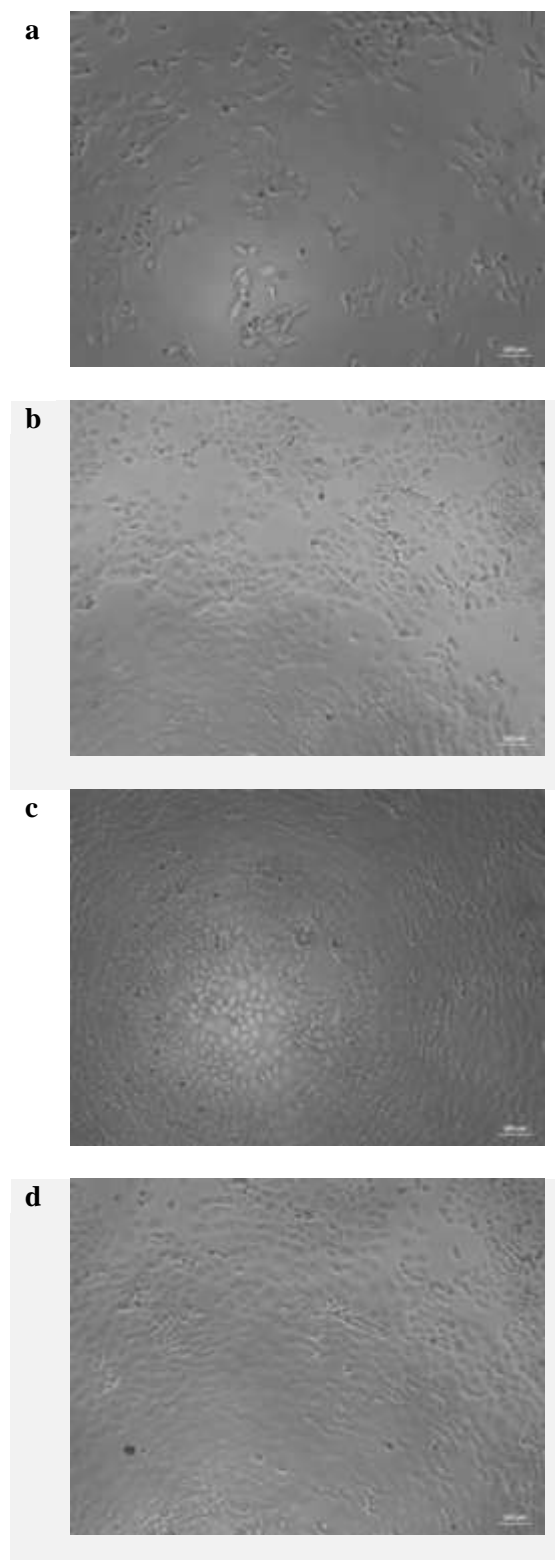

Figure 11. Representative picture of cells at different concentrations of CPH CDs (a) 500 µg/ml (b) 250 µg/ml (c) 125 µg/ml (d) 75 µg/ml (e) 25 µg/ml and (f) MTT assay to determine the percentage of cell viability of Caco2 cells.

4. CONCLUSION

In conclusion, CPH, a biomass waste from the cocoa industry, may be the most cost-effective and readily available precursor for CD synthesis via a simple microwave irradiation method. Our CPH CDs having size of 10-30 nm and rounded in shape. XRD revealed existence of carbon in our CPH CDs based on $2\Theta = 20.71°$. FTIR demonstrated multiple functional chemical groups on the surface of the CPH CDs mainly C=O, N–H and C–N. UV-Vis's absorption spectrum revealed two distinct peaks (235 and 293 nm) and PL spectra of CPH CDs revealed a red shift. Additionally, it was discovered that the green CDs synthesized from CPH do not cause toxicity. Brine shrimp assay indicated that 0.001 mg/ml showed lower lethality percentage. Cytotoxicity evaluation in vitro to determine the

cytotoxicity of CPH CDs was conducted was determined using the MTT assay using human colon adenocarcinoma cells (Caco2). There was a concentration-dependent decrease in viability of Caco2 cell line with IC50 value of 155 ug/ml. Therefore, the results suggested that our CPH CDs are safe for use in bioimaging and drug delivery in the pharmaceutical industry.

ACKNOWLEDGEMENTS

CONFLICT OF INTEREST

The authors declare that they have no conflict of interest.

REFERENCES

1. Boakye-Yiadom, K. O., Kesse, S., Opoku-Damoah, Y., Filli, M. S., Aquib, M., Joelle, M. M. B., Farooq, M.A., Mavlyanova, R., Raza, F., Bavi, R., Wang, B., "Carbon dots: Applications in bioimaging and theranostics", *International journal of pharmaceutics*, 564 (2019) 308-317.
2. Das, P., Ganguly, S., Maity, P. P., Srivastava, H. K., Bose, M., Dhara, S., Bandyopadhyay, S., Das, A. K., Banerjee, S., Das, N. C., "Converting waste *Allium sativum* peel to nitrogen and sulphur co-doped photoluminescence carbon dots for solar conversion, cell labeling, and photobleaching diligences: a path from discarded waste to value-added products", *Journal of Photochemistry and Photobiology B: Biology*, 197 (2019) 111545.
3. Ghosh, S., Ghosal, K., Mohammad, S. A., Sarkar, K., "Dendrimer functionalized carbon quantum dot for selective detection of breast cancer and gene therapy", *Chemical Engineering Journal,* 373 (2019) 468-484.
4. Sun, Z., Chen, Z., Luo, J., Zhu, Z., Zhang, X., Liu, R., Wu, Z. C., "A yellow-emitting nitrogen-doped carbon dots for sensing of vitamin B12 and their cell-imaging". *Dyes and Pigments*, 176 (2020) 108227.
5. Shahshahanipour, M., Rezaei, B., Ensafi, A. A., Etemadifar, Z., "An ancient plant for the synthesis of a novel carbon dot and its applications as an antibacterial agent and probe for sensing of an anti-cancer drug", *Materials Science and Engineering: C*, 98 (2019) 826-833.
6. Shekarbeygi, Z., Farhadian, N., Khani, S., Moradi, S., Shahlaei, M. "The effects of rose pigments extracted by different methods on the optical properties of carbon quantum dots and its efficacy in the determination of Diazinon", *Microchemical Journal*, 158 (2020) 105232.
7. Senol, A. M., Bozkurt, E., "Facile green and one-pot synthesis of seville orange derived carbon dots as a fluorescent sensor for Fe^{3+} ions", *Microchemical Journal*, 159 (2020) 105357.
8. Bhamore, J. R., Jha, S., Park, T. J., Kailasa, S. K., "Green synthesis of multi-color emissive carbon dots from *Manilkara zapota* fruits for bioimaging of bacterial and fungal cells", *Journal of Photochemistry and Photobiology B: Biology*, 191 (2019) 150-155.
9. Ramanarayanan, R., Swaminathan, S. "Synthesis and characterisation of green luminescent carbon dots from guava leaf extract", *Materials Today: Proceedings*, 33 (2020) 2223-2227.
10. Diao, H., Li, T., Zhang, R., Kang, Y., Liu, W., Cui, Y., Wei, S., Wang, N., Li, L., Wang, H., Niu, W., "Facile and green synthesis of fluorescent carbon dots with tunable emission for sensors and cells imaging", *Spectrochimica Acta Part A: Molecular and Biomolecular Spectroscopy*, 200 (2018) 226-234.
11. Zhang, X., Wang, H., Ma, C., Niu, N., Chen, Z., Liu, S., Li, J., Li, S., "Seeking values from biomass materials: Preparation of coffee bean shell-derived fluorescent carbon dots via molecular aggregation for antioxidation and bioimaging applications", *Materials Chemistry Frontiers,* 2(7) (2018) 1269-1275.
12. Costa, R. S., de Castro, M. O., da Silva, G. H., Delite, F. D. S., Strauss, M., Ferreira, O. P., Martinez, D. S. T., Viana, B. C., "Carbon-dots from Babassu coconut (*Orbignya speciosa*) biomass: Synthesis, characterization, and toxicity to Daphnia magna", *Carbon Trends*, (2021) 100133.
13. Liu, L., Quan, M., Sun, H., Yang, Z. Q., Xiao, L., Gong, X., Hu, Q. "A highly sensitive fluorescence probe for methyl parathion detection in vegetable and fruit samples based on N and S co-doped carbon dots" *Journal of Food Composition and Analysis,* (2021) 104374.

14. Paul, A., Kurian, M., "Facile synthesis of nitrogen doped carbon dots from waste biomass: Potential optical and biomedical applications", *Cleaner Engineering and Technology*, 3 (2021) 100103.

15. Tang, C., Long, R., Tong, X., Guo, Y., Tong, C., Shi, S., "Dual-emission biomass carbon dots for near-infrared ratiometric fluorescence determination and imaging of ascorbic acid", *Microchemical Journal*, 164 (2021) 106000.

16. Jayan, S. S., Jayan, J. S., Sneha, B., Abha, K., "Facile synthesis of carbon dots using tender coconut water for the fluorescence detection of heavy metal ions", *Materials Today: Proceedings*, 43 (2021) 3821-3825.

17. Dahunsi, S. O., Adesulu-Dahunsi, A. T., Izebere, J. O., "Cleaner energy through liquefaction of Cocoa (*Theobroma cacao*) pod husk: Pretreatment and process optimization", *Journal of Cleaner Production*, 226 (2019) 578-588.

18. Sanyang, M. L., Sapuan, S. M., Haron, M., "Effect of cocoa pod husk filler loading on tensile properties of cocoa pod husk/polylactic acid green biocomposite films", *AIP Conference Proceedings*, 1891(1) (2017) 020126.

19. Lu, F., Rodriguez-Garcia, J., Van Damme, I., Westwood, N. J., Shaw, L., Robinson, J. S., Warren, G., Chatzifragkou, A., Mason, S. M., Gomez, L., Faas, L., "Valorisation strategies for cocoa pod husk and its fractions", *Current Opinion in Green and Sustainable Chemistry*, 14 (2018) 80-88.

20. Putra, S. S. S., Jimat, D. N., Fazli, W. M., Sulaiman, S., Jamal, P., Nor, Y. A., "Surface functionalisation of microfibrillated cellulose (MFC) of cocoa pod husk with Y-Methacryloxypropyltrimethoxysilane (MPS)", *Materials Today: Proceedings*, 5(10) (2018) 22000-22009.

21. Campos-Vega, R., Nieto-Figueroa, K. H., Oomah, B. D., "Cocoa (*Theobroma cacao L.*) pod husk: Renewable source of bioactive compounds", *Trends in Food Science & Technology*, 81 (2018) 172-184.

22. Dahunsi, S. O., Adesulu-Dahunsi, A. T., Izebere, J. O., "Cleaner energy through liquefaction of Cocoa (*Theobroma cacao*) pod husk: Pretreatment and process optimization", *Journal of Cleaner Production*, 226 (2019) 578-588.

23. Lu, F., Rodriguez-Garcia, J., Van Damme, I., Westwood, N. J., Shaw, L., Robinson, J. S., Warren, G., Chatzifragkou, A., Mason, S. M., Gomez, L., Faas, L., "Valorisation strategies for cocoa pod husk and its fractions", *Current Opinion in Green and Sustainable Chemistry*, 14 (2018) 80-88.

24. Khanahmadi, S., Yusof, F., Ong, H. C., Amid, A., Shah, H., "Cocoa pod husk: A new source of CLEA-lipase for preparation of low-cost biodiesel: An optimized process", *Journal of biotechnology*, 231 (2016) 95-105.

25. Adi-Dako, O., Ofori-Kwakye, K., Manso, S. F., Boakye-Gyasi, M. E., Sasu, C., Pobee, M., "Physicochemical and antimicrobial properties of cocoa pod husk pectin intended as a versatile pharmaceutical excipient and nutraceutical", *Journal of pharmaceutics*, 2016.

26. Ghosal, K., Ghosh, A., "Carbon dots: The next generation platform for biomedical applications. *Materials Science and Engineering C*, 96 (2019) 887-903.

27. Supchocksoonthorn, P., Thongsai, N., Moonmuang, H., Kladsomboon, S., Jaiyong, P., Paoprasert, P., "Label-free carbon dots from black sesame seeds for real-time detection of ammonia vapor via optical electronic nose and density functional theory calculation", *Colloids and Surfaces A: Physicochemical and Engineering Aspects*, 575 (2019) 118-128.

28. Crista, D., Esteves da Silva, J. C., & Pinto da Silva, L., "Evaluation of different bottom-up routes for the fabrication of carbon dots", *Nanomaterials*, 10(7) (2020) 1316.

29. Bruno, F., Sciortino, A., Buscarino, G., Soriano, M. L., Ríos, Á., Cannas, M., Gelardi, F., Messina, F. Agnello, S., "A Comparative Study of Top-Down and Bottom-Up Carbon Nanodots and Their Interaction with Mercury Ions", *Nanomaterials*, 11(5) (2021) 1265.

30. Sharma, A., Das, J., "Small molecules derived carbon dots: synthesis and applications in sensing, catalysis, imaging, and biomedicine", *Journal of Nanobiotechnology*, 17(1) (2019) 1-24.

31. Moradi, S., Sadrjavadi, K., Farhadian, N., Hosseinzadeh, L., Shahlaei, M., "Easy synthesis, characterization and cell cytotoxicity of green nano carbon dots using hydrothermal carbonization of Gum Tragacanth and chitosan biopolymers for bioimaging", *Journal of Molecular Liquids*, 259 (2018) 284-290.

32. Wang, H., Xie, Y., Na, X., Bi, J., Liu, S., Zhang, L., Tan, M., "Fluorescent carbon dots in baked lamb: formation, cytotoxicity and scavenging capability to free radicals", *Food chemistry*, 286 (2019) 405-412.

33. Sendão, R., de Yuso, M. D. V. M., Algarra, M., da Silva, J. C. E., da Silva, L. P., "Comparative life cycle assessment of bottom-up synthesis routes for carbon dots derived from citric acid and urea", *Journal of Cleaner Production*, 254 (2020) 120080.

34. Gusain, D., Renuka, N., Guldhe, A., Bux, F., "Use of microalgal lipids and carbohydrates for the synthesis of carbon dots via hydrothermal microwave treatment", *Inorganic Chemistry Communications*, 134 (2021) 109021.

35. Wu, Y., Li, Y., Pan, X., Hu, C., Zhuang, J., Zhang, X., Lei, B., Liu, Y., "Hemicellulose-triggered high-yield synthesis of carbon dots from biomass", *New Journal of Chemistry*, 45(12) (2021) 5484-5490.

36. Naidu, J. R., Ismail, R., Sasidharan, S., "Acute oral toxicity and brine shrimp lethality of methanol extract of *Mentha Spicata* L (*Lamiaceae*)", *Tropical Journal of Pharmaceutical Research*, 13(1) (2014) 101-107.

37. Raveendran, P. V., Aswathi, B. S., Renuka, N. K., "*Arrowroot derived carbon dots: Green synthesis and application as an efficient optical probe for fluoride ions*", Materials Today: Proceedings, (2021).

38. Dhandapani, E., Duraisamy, N., Periasamy, P., "*Highly green fluorescent carbon quantum dots synthesis via hydrothermal method from fish scale*", Materials Today: Proceedings, (2021)

39. Ganesan, S., Kalimuthu, R., Kanagaraj, T., Kulandaivelu, R., Nagappan, R., Pragasan, L. A., Ponnusamy, V. K., "Microwave-assisted green synthesis of multi-functional carbon quantum dots as efficient fluorescence sensor for ultra-trace level monitoring of ammonia in environmental water", *Environmental research*, (2021) 112589.

40. Siddique, A. B., Pramanic, A. K., Chatterjee, S. Ray, M., "Amorphous carbon dots and their remarkable ability to detect 2,4,6-Trinitrophenol", *Scientific Reports,* 8(1) (2018) 1-10.

41. Atchudan, R., Gangadaran, P., Edison, T. N. J. I., Perumal, S., Sundramoorthy, A. K., Vinodh, R., Rajendran, R. L., Ahn, B. C., Lee, Y. R., "Betel leaf derived multicolor emitting carbon dots as a fluorescent probe for imaging mouse normal fibroblast and human thyroid cancer cells", *Physica E: Low-dimensional Systems and Nanostructures*, 136 (2022) 115010.

42. Tejwan, N., Saha, S. K., Das, J., "Multifaceted applications of green carbon dots synthesized from renewable sources", *Advances in colloid and interface science*, 275 (2020) 102046.

43. Ding, C., Deng, Z., Chen, J., Jin, Y., "One-step microwave synthesis of N, S co-doped carbon dots from 1,6-hexanediamine dihydrochloride for cell imaging and ion detection", *Colloids and Surfaces B: Biointerfaces*, 189 (2020) 110838.

44. Jumardin, J., Maddu, A., Santoso, K., Isnaeni, I., "Synthesis of Carbon Dots (CDS) and Determination of Optical Gap Energy with Tauc Plot Method", *Jambura Physics Journal*, 3(2) (2021) 73-86.

45. Sekar, A., Yadav, R., "Green Fabrication of Zinc Oxide Supported Carbon Dots for Visible Light-Responsive Photocatalytic Decolourization of Malachite Green Dye: Optimization and Kinetic Studies", *Optik*, (2021) 167311.

46. Yu, J., Liu, C., Yuan, K., Lu, Z., Cheng, Y., Li, L., Zhang, X., Jin, P., Meng F., Liu, H., "Luminescence mechanism of carbon dots by tailoring functional groups for sensing Fe3+ ions", *Nanomaterials*, 8(4) (2018) 233.

47. Sutanto, H., Alkian, I., Romanda, N., Lewa, I. W. L., Marhaendrajaya, I., Triadyaksa, P., "High green-emission carbon dots and its optical properties: Microwave power effect", *AIP Advances*, 10(5) (2020) 055008.

48. Abd Rani, U., Ng, L. Y., Ng, C. Y., Mahmoudi, E., "A review of carbon quantum dots and their applications in wastewater treatment", *Advances in colloid and interface science*, 278 (2020) 102124.

49. Man, Y., Li, Z., Kong, W.L., Li, W., Dong, W., Wang, Y., Xie, F., Zhao, D., Qu, Q., Zou, W. S., "Starch fermentation wastewater as a precursor to prepare S, N-doped carbon dots for selective Fe (III) detection and carbon microspheres for solution decolorization", *Microchemical Journal*, 159 (2020) 105338.

50. Jimat, D. N., Talha, N. S., Husin, N. F. C., Azmi, A. S., Raus, R. A., "Screening cellulolytic fungi isolated from Malaysia cocoa pod husk and its culture conditions for cellulase production", *J. Trop. Resour. Sustain. Sci*, 3 (2015) 185-190.

51. Basak, P., Paul, S. and Majumder, R., "Invitro cytotoxic study of aloe vera whole leaf extract on PBMC and breast cancer cell line", *International Conference for Convergence in Technology*, (2017) 124-127

52. Rahmani, A. H., Aldebasi, Y. H., Srikar, S., Khan, A. A., Aly, S. M., "Aloe vera: Potential candidate in health management via modulation of biological activities", *Pharmacognosy Reviews*, 9(18) (2015) 120.

53. Mu'nisa, A., Pagarra, H., Maulana, Z., "Active compounds extraction of cocoa pod husk (Thebroma cacao L.) and potential as fungicides", *Journal of Physics: Conference series*, 1028 (2018) 012013.

Norman, et al.